

# RSC Advances



This is an *Accepted Manuscript*, which has been through the Royal Society of Chemistry peer review process and has been accepted for publication.

*Accepted Manuscripts* are published online shortly after acceptance, before technical editing, formatting and proof reading. Using this free service, authors can make their results available to the community, in citable form, before we publish the edited article. This *Accepted Manuscript* will be replaced by the edited, formatted and paginated article as soon as this is available.

You can find more information about *Accepted Manuscripts* in the [Information for Authors](#).

Please note that technical editing may introduce minor changes to the text and/or graphics, which may alter content. The journal's standard [Terms & Conditions](#) and the [Ethical guidelines](#) still apply. In no event shall the Royal Society of Chemistry be held responsible for any errors or omissions in this *Accepted Manuscript* or any consequences arising from the use of any information it contains.



Journal Name

ARTICLE

## *In-situ* Viscosity Measurement of Confined Liquids

A. Ponjavic,<sup>†ab</sup> J. Dench,<sup>†a</sup> N. Morgan<sup>ac</sup> and J.S.S. Wong<sup>\*a</sup>Received 00th January 20xx,  
Accepted 00th January 20xx

DOI: 10.1039/x0xx00000x

[www.rsc.org/](http://www.rsc.org/)

The viscosity of liquids governs crucial physical and engineering phenomena, ranging from diffusion and transport processes of nutrients and chemicals, to the generation of friction and the physics of damping. Engineering fluids frequently experience local conditions that change their bulk rheological properties. While viscosity data can easily be acquired using conventional rheometers, the results are not always applicable to fluids under engineering conditions. This is particularly the case for fluids being sheared at high pressure under severe confinement, which experience very high shear stresses and often show extensive shear thinning. There is a lack of suitable methods for measuring fluid viscosity under such conditions. This work describes a novel *in-situ* viscosity measurement technique to fill this gap. It involves the quantification of the fluorescence lifetime of a fluorescent dye that is sensitive to viscosity. The capability of the developed technique is verified by taking measurements in submicron thick films of two model fluids confined in a ball on flat contact. Viscosity measurements were successfully performed at pressures up to 1.2 GPa and shear rates up to  $10^5 \text{ s}^{-1}$ . Spatial heterogeneity in viscosity caused by variations in pressure within the thin fluid film could be observed using the technique. It was also possible to detect differences in the rheological responses of a Newtonian and a non-Newtonian fluid. These first *in-situ* high pressure, high shear viscosity measurements demonstrate the versatility of the proposed technique in providing information on the viscosity in conditions where contemporary techniques are insufficient. More importantly it highlights the complexity of the rheology of engineering fluids and provides a means of verifying existing theories by performing *in-situ* measurements. Information on local viscosity is crucial for understanding the physics of confined fluids and to facilitate improvements in engineering technology.

<sup>a</sup> Department of Mechanical Engineering, Imperial College London, SW7 2AZ, UK.  
E-mail: j.wong@imperial.ac.uk

<sup>b</sup> Current address: Department of Chemistry, University of Cambridge, Cambridge, CB2 1EW, UK

<sup>c</sup> Shell Global Solutions (UK) Ltd, Brabazon House, Threapwood Road, Manchester, M22 0RR, UK

<sup>†</sup> These authors contributed equally to this work.

## 1 Introduction

2 The viscosity of a liquid describes its rate of  
3 deformation in response to an applied shear stress.  
4 This property is of great importance in numerous  
5 applications as it affects physical phenomena such as  
6 the diffusion of molecules, the rate of reactions and  
7 the generation of friction.<sup>1</sup> Consequently, the ability  
8 to directly measure the viscosity of liquids is vital for  
9 understanding and controlling these processes.

10 While the viscosity of bulk liquids are usually  
11 measured using rheometers, modern techniques have  
12 been developed to enable probing of previously  
13 inaccessible, highly confined systems such as  
14 nanoscopically thin liquid films. These techniques  
15 include surface forces apparatus,<sup>2</sup> atomic force  
16 microscopy<sup>3</sup> and colloidal probe microscopy.<sup>4</sup> Their  
17 application has led to important discoveries, such as  
18 the confined state of liquids<sup>2,5</sup> and the existence of  
19 boundary slip.<sup>6,7</sup> The main limitation of their use is  
20 the measurement of a single force to describe  
21 properties of the whole liquid film. Large variations  
22 in the local viscosity can exist within both biological  
23 systems, such as in cells,<sup>8,9</sup> and non-conforming  
24 lubricated contacts in engineering systems.<sup>10,11</sup> Such  
25 a lubricated contact, represented by a sphere rubbing  
26 against a flat surface is shown in Fig. 1a. The two  
27 surfaces confine a thin layer of liquid within which  
28 the local pressure varies greatly with position,  
29 reaching peak values in the order of gigapascals.<sup>12</sup>  
30 This causes a large spatial variation in viscosity of  
31 the liquid layer which cannot be studied using a  
32 single force measurement.

33 The combination of very high pressures and large  
34 shear rates (up to  $10^8 \text{ s}^{-1}$ ), can also lead to shear  
35 thinning, where the apparent viscosity of the liquid is  
36 reduced. Shear thinning of liquids has typically been  
37 studied by measuring the overall friction in a  
38 contact<sup>1</sup> or by the use of high pressure rheometers.<sup>13</sup>  
39 Neither of these techniques can be used to study the  
40 spatial variation of viscosity. Spectroscopic  
41 techniques have been developed to provide new  
42 information about the state of liquids in contacts.  
43 These include ultrasonic shear reflection  
44 viscometry,<sup>14</sup> Raman spectroscopy for pressure  
45 sensing<sup>15</sup> and nanoparticle sensors for pressure and  
46 viscosity measurements.<sup>16</sup> Ultrasonic shear reflection  
47 viscometry only provides a spatial resolution of  
48 about  $10 \mu\text{m}$  and the viscosity range studied has been  
49 limited ( $0.1 - 3 \text{ Pa}\cdot\text{s}$ ). Raman spectroscopy can be  
50 used to measure pressure in a contact but the  
51 technique is insensitive to changes in viscosity. The  
52 recently developed nanosensors on the other hand  
53 respond to variations in viscosity, but there is little  
54 information about their sensitivity and the applicable  
55 viscosity range.<sup>16</sup> Here, we propose the use of a  
56 viscosity sensing fluorescent dye, which is a

57 molecular rotor, to measure the viscosity distribution  
58 of liquid in a high pressure contact.

59 A fluorescent molecule emits light when it is excited  
60 by a laser. Molecular rotors are molecules whose  
61 fluorescent properties depend on their surroundings.  
62 They typically have two substructures which can  
63 rotate relative to one another about a shared bond  
64 (see Fig. 2). The ease of this rotation affects the  
65 properties of their fluorescence emission.<sup>17</sup> Hence  
66 the local viscosity, or more specifically the rigidity  
67 of the dye environment, can be probed by measuring  
68 the fluorescence of the molecular rotor. Viscosity  
69 measurements using molecular rotors can be  
70 performed based on fluorescence intensity,<sup>18</sup>  
71 ratiometric methods,<sup>19,20</sup> fluorescence lifetime<sup>21,22</sup> or  
72 anisotropy.<sup>23</sup> Molecular rotors have been used to  
73 study viscosity distributions in cells,<sup>20,22</sup> to observe  
74 the flow of liquids<sup>18,24</sup> and to monitor pressure-  
75 induced viscosity changes of bulk liquids.<sup>25</sup>  
76 However, their use outside the fields of physical  
77 chemistry and biology has been limited. This is  
78 probably because engineering conditions imposed on  
79 liquids, such as high normal pressure and high shear  
80 rates, coupled with limited optical access pose  
81 challenges to the successful application of molecular  
82 rotors for viscosity measurements.

83 In this paper, the capability of molecular rotors to act  
84 as viscosity sensors at high pressure and high shear  
85 conditions is assessed by examining pressure-  
86 induced changes in the viscosity of glycerol and  
87 IGEPAL. Thioflavin T (ThT) is added into the liquid  
88 of interest and the viscosity is examined by  
89 measuring the fluorescence lifetime of ThT. It is  
90 found that the intensity of ThT fluorescence decays  
91 exponentially with time (see Fig. 3). Fluorescence  
92 lifetime corresponds to the characteristic time  
93 constant of this decay. Acquisition of such lifetimes  
94 enables the determination of the relationship between  
95 pressure and viscosity which is then compared to  
96 macroscopic measurements from the literature. In  
97 addition, spatial variations in viscosity and the extent  
98 of shear thinning of confined liquids at high shear  
99 stresses are explored. These applications demonstrate  
100 the power of *in-situ* viscosity measurements using  
101 molecular rotors. This technique can provide insights  
102 on the state of liquids in heterogeneous and highly  
103 confined systems under conditions that cannot be  
104 studied using contemporary methods.

## 105 Experimental

### 106 Materials

107 Thioflavin T (ThT) (T3516), glycerol (G7893), and  
108 IGEPAL CO-520 (238643) were obtained from  
109 Sigma-Aldrich. Glycerol and IGEPAL were chosen  
110 as model Newtonian and shear-thinning liquids. The  
111 chemical structures of glycerol and IGEPAL are

1 depicted in Fig. 2 and their properties are listed in  
2 Table 1.

3 Table 1: Properties of liquids used in this work

	$M_n$ (g/mol)	$\eta$ (Pa·s)	$\alpha$ (GPa <sup>-1</sup> )
Glycerol	92.1	1.135 <sup>a</sup>	6.5 <sup>c</sup>
IGEPAL CO-520	441	0.23 <sup>b</sup>	g <sup>c</sup>

4 <sup>a</sup> Data at 22.5° taken from <sup>26</sup> <sup>b</sup> Viscosity at 25°C determined using a  
5 cylindrical viscometer. <sup>c</sup> Based on exponential fit to experimental  
6 data from friction measurements.  $M_n$ : Molecular weight,  $\eta$ :  
7 viscosity,  $\alpha$ : Pressure-viscosity coefficient.

8 ThT is the dye molecule chosen as a model viscosity  
9 sensor in this study. It is a molecular rotor that has  
10 found widespread use in biophysics for the  
11 identification of misfolded proteins,<sup>27</sup> which are  
12 thought to be linked to neurodegenerative diseases  
13 such as Alzheimer's. The fluorescence emission of  
14 ThT in low viscosity solutions such as water is very  
15 weak. The rotation of the benzthiazole and  
16 diaminobenzene fragments (see Fig. 2) facilitates  
17 photoinduced twisted intramolecular charge  
18 transfer,<sup>21</sup> which quenches the fluorescence of the  
19 dye molecule. Restricting the rotation of these  
20 fragments upon binding to protein  $\beta$ -sheets, or due to  
21 an increase in solvent viscosity, causes up to a  
22 hundred-fold increase in the quantum yield of the  
23 rotor<sup>28</sup> and a corresponding increase in its  
24 fluorescence lifetime. This is due to the intrinsic link  
25 between the quantum yield and the fluorescent  
26 lifetime.<sup>23</sup>

27 Unlike Raman scattering,<sup>15</sup> ThT lifetime is affected  
28 by changes in viscosity rather than pressure. The  
29 fluorescence lifetime of ThT has been shown to be  
30 related to the viscosity of glass-forming liquids.<sup>28</sup>  
31 Furthermore, pressure-induced changes in viscosity  
32 have been observed using this molecular rotor.<sup>25</sup>  
33 However, the relationship between fluorescence  
34 lifetime and viscosity is not straightforward as the  
35 quenching of ThT may involve multiple processes,  
36 which somewhat complicates its use as a viscosity  
37 sensor. Nevertheless, its insensitivity to pressure  
38 makes it ideal for examining liquid viscosity in a  
39 point contact where there is a very large spatial  
40 variation of pressure.

41 Test liquids were prepared by dissolving ThT into  
42 glycerol or IGEPAL under magnetic stirring at 55°C  
43 for at least an hour. The final ThT concentration of  
44 the solutions after filtration through a 1  $\mu$ m filter  
45 (514-4027 Syringe filters, Acrodisc®, glass fibre  
46 VWR), was about 1.7 mM. This relatively high ThT  
47 concentration is required due to the limited  
48 fluorescence emission from the sub-micron thin  
49 films tested in this study.

50 As the liquids are hygroscopic, tests were carried out  
51 as soon as possible after depositing fresh liquid to  
52 limit changes in viscosity caused by water  
53 absorption.

#### 54 High pressure, high shear viscometry in a point contact

55 In order to investigate the rheology of submicron  
56 thick engineering fluids at high pressure and high  
57 shear conditions, a compact rheometer was  
58 developed based on a lubricated point contact. The  
59 experimental platform consists of a point contact  
60 created by a ball rubbing against a flat disc surface  
61 (see Fig. 1a). A thin layer of test liquid is spread on  
62 the flat surface. When the ball is loaded against the  
63 flat surface under relative motion, elastic  
64 deformation of the rubbing surfaces creates a locally-  
65 flattened region. This enables the formation of a  
66 separating, confined liquid film of almost constant  
67 thickness (see Fig. 1b). The rotational speeds of the  
68 ball,  $u_b$ , and the disc,  $u_d$ , are controlled separately.  
69 The entrainment speed,  $u_e = (u_b + u_d)/2$ , i.e. the  
70 mean speed at which liquid enters the contact,  
71 governs the thickness of the confined film,  $h$ , so that  
72 a combination of  $u_b$  and  $u_d$  that maintains  $u_e$  results  
73 in the same film thickness. Hence the shear rate,  
74  $\dot{\gamma} = (u_b - u_d)/h$ , can be controlled by varying the  
75 relative speed of the ball and disc, while keeping  $u_e$   
76 and hence  $h$  constant.

77 The load is applied as a dead weight. The position, of  
78 the observation volume in the contact at which local  
79 viscosity is measured, was controlled using an  
80 automated microscope stage. The stabilities of this  
81 position and its intensity were about 5  $\mu$ m and 5 %  
82 respectively.

83 Three types of ball materials (glass, AISI52100 steel  
84 and tungsten carbide) and two transparent flats (glass  
85 and sapphire) were employed to cover a wide range  
86 of contact pressures. The experimental conditions are  
87 listed in Table 2. All experiments were performed at  
88 a room temperature of 21-23°C.

89 Table 2: Experimental conditions

Pressure, $P$ (GPa)	0.2 – 1.2
Film thickness, $h$ (nm)	100 – 300
Shear rate, $\dot{\gamma}$ (s <sup>-1</sup> )	$1 \times 10^4 - 5 \times 10^5$

90 The normal pressure exerted on the confined liquid,  
91  $P$ , in a point contact depends on its relative position  
92 in the contact.  $P$  is commonly assumed to obey the  
93 stationary Hertzian parabolic pressure distribution:

$$94 \quad P(r) = P_{max} \left(1 - \frac{r^2}{a^2}\right)^{1/2} \quad (1)$$

95 where  $r$  is the distance from the centre of the contact  
96 and  $a$  is the radius of the contact.  $P_{max}$  is the peak  
97 pressure and is equal to

$$98 \quad P_{max} = \frac{3W}{2\pi a^2} \quad (2)$$

1 where  $W$  is the applied point load.  $a$  was measured  
2 using optical interferometry, except for the cases of  
3 glass ball against glass disc contacts, where  
4 reflections on the glass surfaces are negligible. A  
5 correction based on the measured  $a$  and the  
6 theoretical Hertzian  $a$  from steel ball against glass  
7 disc contacts was applied to glass ball against glass  
8 disc contacts to obtain the correct pressure.

9 The film thickness of the liquid in an EHD contact  
10 was measured with optical interferometry<sup>29</sup> using an  
11 EHD2 ultrathin film measurements system (PCS  
12 instruments). The film thickness measurements were  
13 used to calculate the average applied shear rate.  
14 Friction measurements taken using a MTM2 Mini  
15 Traction Machine (PCS Instruments) were used to  
16 compute the average shear stress. This enabled  
17 calculation of the pressure viscosity coefficient,  $\alpha$ ,  
18 using the average strain rate obtained with film  
19 thickness measurements.

### 20 Lifetime measurement

21 If a molecular rotor is dissolved in the entrained  
22 liquid, the effect of applied pressure on the local  
23 viscosity can be investigated by measuring the  
24 lifetime of the fluorescence emission produced by  
25 the molecular rotor. As the viscosity of the liquid  
26 increases due to pressure, so does the lifetime. Thus  
27 longer lifetimes would be expected in the central  
28 region of the contact where the pressure is largest,  
29 (see Fig. 1b). The use of a point contact as a  
30 rheometer thus allows the effect of pressure  
31 heterogeneity on viscosity to be examined.

32 The experimental platform was placed on an inverted  
33 microscope where a laser beam at 400 nm was  
34 directed into the confined liquid to excite the dye in  
35 the model lubricant. The laser used was a  
36 femtosecond Ti:Sapphire laser (Tsunami, Spectra  
37 Physics), which was pumped by a 5W 532 nm laser.  
38 The output wavelength was set to 800 nm with a  
39 repetition rate of 80 MHz and a pulse width of about  
40 80 fs. It was then frequency-doubled, resulting in a  
41 wavelength of 400 nm, with residual 800 nm  
42 radiation filtered using a 750 nm short pass filter.  
43 This 400 nm beam was then expanded, collimated,  
44 and directed into the confined liquid through an  
45 objective (20x Olympus UPlanFL N, NA=0.5) using  
46 a dichroic mirror. The emission of the dye was  
47 collected by the same objective, passing through  
48 long pass filters to remove the excitation beam, and a  
49 tube lens, after which it was acquired using a single  
50 photon avalanche photodiode. The lifetime of ThT in  
51 the studied liquids was measured by time-correlated  
52 single photon counting (TCSPC) using an SPC-152  
53 (Becker & Hickl) TCSPC module. The TCSPC  
54 module was connected to the output of the single  
55 photon avalanche photodiode and the  
56 synchronisation signal from the laser controller. The  
57 instrument response function of the system had a full

58 width half maximum of 80 ps induced by limitations  
59 of the avalanche photodiode.

60 Care must be taken to limit laser heating of the  
61 liquid. Experiments with various laser powers and  
62 dye concentrations in model liquids were conducted  
63 to examine the effect of laser heating (results not  
64 shown). By selecting the appropriate dye  
65 concentration and laser power, the effect of laser  
66 heating could be avoided.

67 As described in the introduction, viscosity  
68 measurements using molecular rotors can be  
69 intensity (absolute/ratiometric) or lifetime based.  
70 Lifetime measurement was chosen over fluorescence  
71 emission intensity because the lifetime of ThT does  
72 not depend on film thickness, which changes with  
73 the entrainment speed, or on the chosen geometry of  
74 the experimental platform. In addition, lifetime based  
75 measurements allows viscosity to be measured with  
76 high spatial resolution. The spatial resolution is  
77 defined in this case by the size of the laser beam  
78 exciting the molecular rotor. This is typically limited  
79 to a few hundred nanometers due to the diffraction  
80 limit, but can potentially be surpassed using  
81 stimulated emission depletion.<sup>30</sup>

### 82 Analysis of lifetime data

83 The analysis of ThT lifetime data requires fitting of a  
84 model. A variety of models have been used to  
85 describe the lifetime of ThT.<sup>21,28,31</sup> These all have in  
86 common that they describe a distribution of  
87 lifetimes. The stretched exponential<sup>21,28</sup> is frequently  
88 used to describe the lifetime of molecular rotors with  
89 complex quenching mechanisms.<sup>32</sup> It is defined as

$$90 \quad I(t) = Ae^{-(t/\tau)^n} \quad (3)$$

91 where  $I$  is the intensity at time  $t$ ,  $\tau$  is the lifetime and  
92  $n$  is an exponent. This was fitted to the experimental  
93 fluorescence decay measurements (see Fig. 3). The  
94 characteristic decay time,  $\tau$ , of ThT was then  
95 extracted to obtain the local viscosity. At  
96 atmospheric conditions the exponent  $n$  is between  
97 0.8 – 0.9 in this work. As the fluid becomes more  
98 viscous, the exponent  $n$  tends to unity.

### 99 Lifetime-viscosity calibration

100 The effect of viscosity on the lifetime of ThT was  
101 calibrated using a custom pressure cell, which  
102 allowed the test liquids to be pressurised  
103 hydrostatically from 0 – 650 MPa. All test liquids  
104 were stored in desiccators and were added to the  
105 pressure cell immediately before the test to minimise  
106 water contamination.

107 Once the pressure cell was filled and a desired  
108 pressure was reached, it was left to stabilise for  
109 around 40 s before a lifetime measurement was  
110 taken. The pressure cell had two windows  
111 perpendicular to one another. The ThT-doped liquid



1 was excited through one of the windows, and the  
 2 fluorescence emission was collected through the  
 3 second window. Fluorescence collection and lifetime  
 4 extraction was conducted as described in the  
 5 previous section. The relationship between the  
 6 lifetime of ThT in glycerol and the applied pressure  
 7 was linear as shown in Fig. 4a (solid symbols). This  
 8 relationship was combined with pressure-viscosity  
 9 data from the literature<sup>26</sup> to obtain the relationship  
 10 between the viscosity of glycerol and the lifetime of  
 11 ThT (open circles in Fig. 4a insert). This viscosity-  
 12 lifetime calibration enabled the determination of  
 13 local viscosity based on ThT lifetime in the confined  
 14 liquid film.

15 A similar linear lifetime-pressure relationship is  
 16 obtained for IGEPAL (solid symbols, Fig. 4b). While  
 17 the viscosity of IGEPAL is about 5 to 10 times lower  
 18 than that of glycerol in ambient conditions, ThT has  
 19 a long lifetime in IGEPAL. No direct conversion  
 20 between lifetime and viscosity could be carried out  
 21 since no pressure-viscosity data is available for  
 22 IGEPAL.

## 23 Results and discussion

### 24 Pressure-viscosity relationships using fluorescence 25 lifetime measurement

26 Thin films of ThT-doped Glycerol were entrained in  
 27 a rolling/sliding ball on flat contact. The effect of  
 28 pressure on the viscosity of these films was  
 29 examined by measuring ThT fluorescence lifetime at  
 30 various applied loads. This determined the range of  
 31 viscosities that could be measured using the  
 32 proposed technique, as well as the accuracy of these  
 33 measurements.

34 The fluorescence lifetime of ThT in a confined  
 35 glycerol film was acquired in pure rolling conditions  
 36 ( $u_b = u_d = u_e = 74$  mm/s) at the centre of the  
 37 contact ( $x = y = 0$ ) where the pressure is largest  
 38 (see Fig. 1b). The applied pressure ranged from 200  
 39 MPa to 1.2 GPa, which is similar to pressures  
 40 commonly encountered in engineering components  
 41 such as bearings and gears. For these experimental  
 42 conditions, the film thickness is about 170 nm and  
 43 the liquid does not experience any significant shear  
 44 stress. The lifetime of ThT at various pressures, and  
 45 the corresponding viscosity of glycerol deduced from  
 46 the calibration shown in Fig. 4a are presented in Fig.  
 47 5 (unfilled symbols). Fig. 5 also shows the bulk  
 48 glycerol viscosity obtained from the pressure cell  
 49 experiments (solid squares). The relationship  
 50 between pressure and viscosity at moderate pressures  
 51 (less than 1 GPa) can be described by the Barus  
 52 relationship, which is given by

$$53 \quad \eta = \eta_0 e^{\alpha P} \quad (4)$$

54 where  $\eta$  is the viscosity,  $\eta_0$  is the viscosity at  
 55 ambient pressure,  $\alpha$  is the pressure-viscosity  
 56 coefficient and  $P$  is the pressure. If equation (4) can  
 57 be used to describe glycerol in our test conditions, a  
 58 straight line is expected when the logarithm of the  
 59 viscosity ( $\log(\eta)$ ) is plotted against the applied  
 60 pressure (Fig. 5b). This is observed for hydrostatic  
 61 measurements within the pressure cell (solid  
 62 symbols) where both the lifetime of ThT and  $\log(\eta)$   
 63 are linearly proportional to applied pressure.

64 In a rolling contact, the local viscosity of a confined  
 65 glycerol film increases with pressure and results  
 66 obtained with different material pairs (unfilled  
 67 symbols, see legends in Fig. 5) overlap. This shows  
 68 that the measured viscosity is a direct function of  
 69 pressure and is not affected by the properties of the  
 70 confining surfaces. These values are however lower  
 71 than values taken in the pressure cell (solid symbols  
 72 in Fig. 5). This is not caused by ThT being  
 73 insensitive to high viscosity as a similar range of  
 74 viscosities was observed in the pressure cell  
 75 experiments (unfilled symbols, Fig. 5).

76 Glycerol is a well-known Newtonian liquid. As tests  
 77 in a point contact were conducted under pure rolling  
 78 conditions it is very unlikely that the difference in  
 79 glycerol properties in a pressure cell and in a rolling  
 80 contact is due to shear thinning. Glycerol is also  
 81 hygroscopic, meaning that its viscosity drops with  
 82 time once it is in contact with ambient atmosphere.  
 83 While test liquids were stored in a desiccator, some  
 84 changes in glycerol viscosity could still occur. Since  
 85 glycerol has no contact with air once it is in the  
 86 pressure cell, the issue of water absorption is  
 87 minimised in the calibration experiments. However  
 88 for the rolling contact experiments, a thin layer of  
 89 glycerol was spread on the disc, exposing a large  
 90 surface area. This is likely to promote water  
 91 absorption. This may result in a reduction in glycerol  
 92 viscosity before glycerol enters the contact during  
 93 the confined glycerol experiments. Control  
 94 experiments on how ThT lifetime in confined  
 95 glycerol changes over time were conducted and a  
 96 reduction of ThT lifetime was observed. The lifetime  
 97 of ThT in confined neat glycerol dropped  
 98 significantly over 15 minutes resulting in a lifetime  
 99 equivalent to that of glycerol with 7 wt% water  
 100 (results not shown). The increased exposure to  
 101 ambient atmosphere and hence an increased amount  
 102 of absorbed water in glycerol in the rolling contact  
 103 experiments may explain the lower than expected  
 104 viscosity, and its deviation from the Barus  
 105 relationship.

106 ThT lifetime in confined IGEPAL in a pure rolling  
 107 contact and bulk IGEPAL in the pressure cell are  
 108 compared in Fig. 4b. The two sets of data match  
 109 well, showing that the use of ThT lifetime enables  
 110 the investigation of viscosity in a confined film. Note  
 111 that IGEPAL is not as susceptible to water

1 absorption as glycerol. This supports the observed  
2 discrepancies in data for glycerol in bulk and  
3 glycerol in confinement is due to absorbed water.  
4 At high applied pressures, ThT lifetimes of both  
5 confined glycerol and IGEPAL deviates from  
6 measurements taken from their bulk counterparts.  
7 This may be due to uncertainties in area estimation  
8 and applied pressure at high load conditions. The  
9 actual normal pressure could be lower and hence, the  
10 differences in ThT lifetime in confined and bulk  
11 liquid at high load may be smaller than those  
12 presented Fig. 4b and Fig. 5.  
13 The results show the range of viscosities and  
14 pressures that can be studied using ThT and the  
15 point-contact-based viscometer. It verifies the  
16 suitability of the proposed fluorescence lifetime  
17 measurement for measuring the viscosity of  
18 submicron thick films at high pressures and high  
19 shear conditions.

#### 20 Spatial viscosity distribution in a confined film

21 The pressure experienced by confined liquids in a  
22 point contact is position-dependent. Hence spatial  
23 viscosity heterogeneity is expected in such confined  
24 liquids. Local viscosity mapping can be conducted in  
25 one or two dimensions. The two-dimensional ThT  
26 lifetimes and the corresponding viscosity  
27 distributions of confined glycerol films at peak  
28 pressure,  $P_{max} = 530$  MPa in pure rolling conditions  
29 ( $u_b = u_d = u_e = 74$  mm/s) are shown in Fig. 6a and  
30 Fig. 6b respectively. The one-dimensional ThT  
31 lifetime plots in the  $x$ -direction, along the centre of  
32 the contact (dashed line as shown in Fig. 6a), are also  
33 presented in Fig. 7a (squares). Large spatial  
34 variations within the contact are observed. The local  
35 ThT lifetime (Fig. 6a, and Fig. 7a) and hence  
36 viscosity (Fig. 6b) increases as glycerol travels from  
37 the inlet towards the centre of the contact. They then  
38 drop as glycerol approaches the outlet of the contact.  
39 These distributions have near circular symmetry as  
40 expected from a Hertzian pressure distribution as  
41 described by equation (1). The size of the region  
42 where lifetime and hence viscosity heterogeneity is  
43 detected compares well with the measured contact  
44 size of  $2a = 150$   $\mu\text{m}$  (dashed circle in Fig. 6a). The  
45 local viscosity of confined glycerol in this loading  
46 condition ranges from 0.5 to 8 Pa·s. Note the lifetime  
47 distribution does not show a large increase with  
48 pressure compared to the viscosity rise. This is  
49 because lifetime increases linearly while viscosity  
50 increases exponentially with pressure. Hence ThT  
51 lifetime seems to plateau around the centre of the  
52 contact while viscosity continues to rise and peaks at  
53 around  $x = 0$ .  
54 The effect of pressure is further analysed using one-  
55 dimensional ThT lifetime plots (Fig. 7a) taken along the  
56  $x$ -direction along the centre of the contact (dashed line as  
57 shown in Fig. 6a) for various loading conditions.

58 Raising the applied pressure from  $P_{max} = 530$  MPa  
59 (squares in Fig. 7a) to  $P_{max} = 980$  MPa (triangles in  
60 Fig. 7a) gives rise to an overall increase in the ThT  
61 lifetime (hence viscosity) distribution. Note that the  $x$ -  
62 position where the same pressure level is reached differs  
63 for different loads. In addition, the  $x$ -position defines  
64 the duration the liquid has been in the contact. This  
65 is related to the relaxation of the liquid. When plotting  
66 local ThT lifetime against the local normal pressure  
67 estimated using the Hertzian pressure distribution  
68 (equation (1)) for various loading conditions (under pure  
69 rolling conditions), they all overlap (see Fig. 7b). Fig.  
70 7b suggests that the observed variations in lifetime  
71 (hence viscosity) of confined glycerol is pressure-  
72 induced and no aging effect is observed. This  
73 demonstrates the validity of the applied methodology in  
74 detecting local viscosity heterogeneity.

#### 75 Effects of shear rate on local viscosity of confined 76 liquids

77 Liquids in lubricated non-conforming contacts are  
78 exposed to both high pressures and high shear rates.  
79 For many liquids this can lead to a reduction in  
80 viscosity with shear rate, a phenomenon called shear  
81 thinning. The local ThT lifetime of glycerol and  
82 IGEPAL films at the centre of a ball on flat contact  
83 was examined at various shear rates. Glycerol shows  
84 constant lifetime, hence constant viscosity  
85 throughout the range of tested shear rates (Fig. 8a).  
86 This is consistent with glycerol behaving as a  
87 Newtonian liquid,<sup>33</sup> over the range of pressures and  
88 shear rates examined. By contrast IGEPAL  
89 undergoes shear thinning (Fig. 8b) as shown by a  
90 reduction in ThT lifetime as shear rate increases.  
91 The effect of shear thinning is more pronounced as  
92 pressure increases. This observation is consistent  
93 with behaviour of other shear thinning liquids.<sup>34</sup> The  
94 average viscosity for both liquids at various  
95 pressures was also obtained with friction  
96 measurements (results not shown). Qualitatively  
97 similar behaviour was observed. These results  
98 indicate that fluorescence lifetime measurements are  
99 capable of differentiating liquid behaviour at high  
100 pressure and high shear conditions.  
101 Since the fluorescence lifetime of ThT depends on  
102 the rigidity of its environment, how ThT lifetime  
103 changes with the shear rate can provide information  
104 on how the structure of the test liquid evolves. This  
105 is crucial for identifying the origins of phenomena  
106 such as shear thinning observed with IGEPAL.  
107 IGEPAL is a non-ionic surfactant with  
108 polyoxyethylene (EO) head groups, consisting of 5  
109 EO residues, and a hydrophobic tail. It forms a  
110 structure to minimise contact between EO groups  
111 and hydrophobic groups. In ambient conditions this  
112 may result in a polydomain structure (for example  
113 lots of small multi-layer domains or multi-laminar  
114 vesicles) or a laminar structure.<sup>35</sup> Shear thinning

1 depends on rearrangement of liquid molecules in  
2 response to applied pressure and shear. In the case of  
3 IGEPAL, the type and size of domains<sup>36,37</sup> and  
4 degree of ordering<sup>38,39</sup> are governed by the applied  
5 shear rate. Note that ThT is a cationic dye which may  
6 reside on the EO residual layers within the IGEPAL  
7 layers. Its dimethyl amino group, and possibly the  
8 benzene ring can reside in hydrophobic layers as has  
9 been observed for a similar dye Safranin T.<sup>40</sup> Hence  
10 the results in Fig. 8 suggest that the microstructural  
11 change in IGEPAL is accompanied by a reduction in  
12 rigidity of surfactant layers, which has been  
13 successfully detected by ThT lifetime measurements.  
14 This highlights the unique capability provided by the  
15 combination of friction and fluorescence lifetime  
16 measurements in terms of improving our  
17 understanding of the origins of friction and  
18 rheological changes of confined lubricants.

## 19 Conclusions

20 The use of molecular rotor lifetime measurements  
21 enables the probing of viscosity, with a high spatial  
22 resolution in inaccessible geometries, in a fashion  
23 that cannot be achieved using mechanical methods.  
24 Depending on the dye, the viscosity range can span  
25 multiple orders of magnitude. The combination of  
26 these features, together with the use of a point-  
27 contact-based high pressure, high shear viscometer,  
28 makes the method particularly suitable for  
29 engineering applications.

30 By measuring the local viscosity of confined  
31 Newtonian and shear thinning liquids, it was shown  
32 that molecular rotors can be used to monitor pressure  
33 and shear induced changes in viscosity. For the first  
34 time, local viscosity measurements have been  
35 performed in a confined thin film where the viscosity  
36 heterogeneity/distribution has been quantified. More  
37 importantly, the measurements were the first to be  
38 conducted at simultaneous high pressure (up to 1.2  
39 GPa) and high shear (up to  $\dot{\gamma} = 10^5$ ) conditions with  
40 significant engineering relevance, specifically in  
41 fuels and lubricants. This also has the potential to  
42 resolve issues in the field of physics of liquids where  
43 phenomena such as slip<sup>6,41,42</sup> and confinement<sup>5,43</sup>  
44 have sparked controversies in terms of the accuracy  
45 of experimental methods. Fluorescence lifetime  
46 imaging with molecular rotors could for example be  
47 used to verify the accuracy of models for  
48 hydrodynamic drainage forces<sup>44</sup> used to measure  
49 friction in these systems.<sup>45</sup>

50 In the field of tribology the technique could be used  
51 to reconcile the debate concerning the most  
52 appropriate rheological model to describe lubricant  
53 behaviour in non-conforming contacts.<sup>46</sup> Currently,  
54 this is done by measuring the average friction in  
55 contacts or with high-pressure rheometers. Neither of

56 these can determine the viscosity distribution in a  
57 contact at the relevant conditions. Establishing the  
58 accuracy of models would serve to optimise the  
59 design of lubricants and tribological systems leading  
60 to reductions in energy use. The method could also  
61 be used to probe the viscosity of mixtures which  
62 plays an important role where fuel meets lubricant at  
63 the top piston ring reversal point, in an engine, as  
64 well as in many other drivetrain systems. It should be  
65 noted that the addition of a robust calibration method  
66 to account for potentially differing lifetime/viscosity  
67 relationships of the differing solvents may be  
68 required.

69 These are just a few applications where this  
70 technique could become a useful tool for improving  
71 models describing the state of liquids. Given the vast  
72 amount of applications where viscosity plays a  
73 significant role the developed *in-situ* rheometry  
74 technique will have a great impact in both physics  
75 and engineering.

## 76 Acknowledgments

77 This work is supported by EPSRC research grant no.  
78 EP/J015385/1, and EP/L023202/1. JD is supported by the  
79 Shell University Technology Centre for Fuels and  
80 Lubricants at Imperial College London. The authors  
81 gratefully acknowledge Dr Changki Min and Dr Mourad  
82 Chennaoui for help in the design of frequency doubler  
83 and mechanical devices respectively; and Prof Hugh  
84 Spikes and Dr Luca di Mare for very fruitful discussions.

## 85 Notes & references

- 86 1. C. Evans and K. Johnson, *Proc. Inst. Mech. Eng.*  
87 *Part C J. Mech. Eng. Sci.*, 1986, **200**, 303–312.
- 88 2. J. N. Israelachvili and S. J. Kott, *J. Chem. Phys.*,  
89 1988, **88**, 7162.
- 90 3. N. Ahmed, D. F. Nino, and V. T. Moy, *Rev. Sci.*  
91 *Instrum.*, 2001, **72**, 2731.
- 92 4. O. I. Vinogradova and G. E. Yakubov, *Langmuir*,  
93 2003, **19**, 1227–1234.
- 94 5. H. W. Hu and S. Granick, *Science*, 1992, **258**,  
95 1339–42.
- 96 6. S. Granick, Y. Zhu, and H. Lee, *Nat. Mater.*, 2003,  
97 **2**, 221–227.
- 98 7. E. Bonaccorso, M. Kappl, and H.-J. Butt, *Phys.*  
99 *Rev. Lett.*, 2002, **88**, 1–4.
- 100 8. K. Luby-Phelps, S. Mujumdar, R. B. Mujumdar,  
101 L. A. Ernst, W. Galbraith, and A. S. Waggoner,  
102 *Biophys. J.*, 1993, **65**, 236–42.
- 103 9. B. A. Nemet, Y. Shabtai, and M. Cronin-Golomb,  
104 *Opt. Lett.*, 2002, **27**, 264–266.
- 105 10. B. J. Hamrock and D. Dowson, *J. Lubr. Technol.*,  
106 1977, **99**, 264.



11. M. Hartinger, M.-L. Dumont, S. Ioannides, D. Gosman, and H. Spikes, *J. Tribol.*, 2008, **130**, 041503.
12. A. Erdemir, *Surf. Coatings Technol.*, 1992, **54-55**, 482–489.
13. S. Bair, *Proc. Inst. Mech. Eng. Part J J. Eng. Tribol.*, 2001, **215**, 223–233.
14. S. Kasolang and R. S. Dwyer-Joyce, *Proc. Inst. Mech. Eng. Part J J. Eng. Tribol.*, 2008, **222**, 423–429.
15. I. Jubault, J. L. Mansot, P. Vergne, and D. Mazuyer, *J. Tribol.*, 2002, **124**, 114.
16. H. Hamza, S. M. B. Albahrani, G. Guillot, M. Maillard, D. Philippon, P. Vergne, and J. M. Bluet, *J. Phys. Chem. C*, 2015, **119**, 16897–16904.
17. M. K. Kuimova, *Phys. Chem. Chem. Phys.*, 2012, **14**, 12671–86.
18. M. a. Haidekker, W. Akers, D. Lichlyter, T. P. Brady, and E. a. Theodorakis, *Sens. Lett.*, 2005, **3**, 42–48.
19. M. A. Haidekker, T. P. Brady, D. Lichlyter, and E. A. Theodorakis, *J. Am. Chem. Soc.*, 2006, **128**, 398–9.
20. M. K. Kuimova, S. W. Botchway, A. W. Parker, M. Balaz, H. A. Collins, H. L. Anderson, K. Suhling, and P. R. Ogilby, *Nat. Chem.*, 2009, **1**, 69–73.
21. V. I. Stsiapura, A. A. Maskevich, V. A. Kuzmitsky, V. N. Uversky, I. M. Kuznetsova, and K. Turoverov, *J. Phys. Chem. B*, 2008, **112**, 15893–902.
22. M. K. Kuimova, G. Yahioğlu, J. A. Levitt, and K. Suhling, *J. Am. Chem. Soc.*, 2008, **130**, 6672–3.
23. J. a Levitt, P.-H. Chung, M. K. Kuimova, G. Yahioğlu, Y. Wang, J. Qu, and K. Suhling, *ChemPhysChem*, 2011, **12**, 662–72.
24. M. a Haidekker and E. a Theodorakis, *Org. Biomol. Chem.*, 2007, **5**, 1669–78.
25. N. Amdursky, R. Gepshtein, Y. Erez, N. Koifman, and D. Huppert, *J. Phys. Chem. A*, 2011, **115**, 6481–7.
26. R. L. Cook, C. A. Herbst, and H. E. King, *J. Phys. Chem.*, 1993, **97**, 2355–2361.
27. T. Ban, D. Hamada, K. Hasegawa, H. Naiki, and Y. Goto, *J. Biol. Chem.*, 2003, **278**, 16462–5.
28. N. Amdursky, R. Gepshtein, Y. Erez, and D. Huppert, *J. Phys. Chem. A*, 2011, **115**, 2540–8.
29. R. Glovnea, A. Forrest, A. Olver, and H. Spikes, *Tribol. Lett.*, 2003, **15**, 217–230.
30. S. W. Hell and J. Wichmann, *Opt. Lett.*, 1994, **19**, 47–780.
31. P. K. Singh, M. Kumbhakar, H. Pal, and S. Nath, *J. Phys. Chem. B*, 2010, **114**, 5920–7.
32. K. C. Lee, J. Siegel, S. E. Webb, S. Lévêque-Fort, M. J. Cole, R. Jones, K. Dowling, M. J. Lever, and P. M. French, *Biophys. J.*, 2001, **81**, 1265–74.
33. K. Schröter and E. Donth, *J. Chem. Phys.*, 2000, **113**, 9101.
34. S. Bair, *Proc. Inst. Mech. Eng. Part J J. Eng. Tribol.*, 2002, **216**, 1–17.
35. D. J. Mitchell, G. J. T. Tiddy, L. Waring, T. Bostock, and M. P. McDonald, *J. Chem. Soc. Faraday Trans. 1 Phys. Chem. Condens. Phases*, 1983, **79**, 975.
36. J. Zipfel, F. Nettesheim, P. Lindner, T. D. Le, U. Olsson, and W. Richtering, *Europhys. Lett.*, 2001, **53**, 335–341.
37. T. D. Le, U. Olsson, K. Mortensen, J. Zipfel, and W. Richtering, *Langmuir*, 2001, **17**, 999–1008.
38. O. Diat, D. Roux, and F. Nallet, *Phys. Rev. E*, 1995, **51**, 3296–3299.
39. P. Sierro and D. Roux, *Phys. Rev. Lett.*, 1997, **78**, 1496–1499.
40. S. K. Ghosh, P. K. Khatua, and S. C. S. C. Bhattacharya, *J. Colloid Interface Sci.*, 2004, **275**, 623–31.
41. R. Pit, H. Hervet, and L. Léger, *Phys. Rev. Lett.*, 2000, **73**, 2000.
42. D. Lumma, A. Best, A. Gansen, F. Feuillebois, and J. O. Rädler, and O. I. Vinogradova, *Phys. Rev. E*, 2003, **67**, 056313.
43. A. Cuenca and H. Bodiguel, *Phys. Rev. Lett.*, 2013, **110**, 108304.
44. O. I. Vinogradova, *Langmuir*, 1995, **11**, 2213–2220.
45. H. Spikes and S. Granick, *Langmuir*, 2003, **19**, 5065–5071.
46. H. Spikes and Z. Jie, *Tribol. Lett.*, 2014, **56**, 1–25.

1

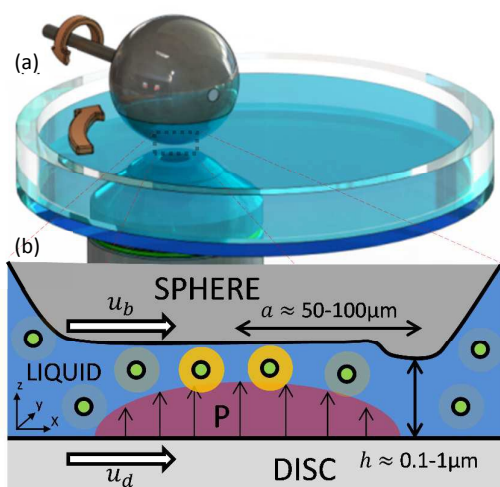


Fig. 1: Schematic showing liquid confined within a nominally point contact. (a) A contact is created by a sphere rubbing against a flat surface. Both the sphere and the disc can rotate independently, at speeds  $u_b$  and  $u_d$ , causing liquid to be entrained and confined between them. (b) Section view along the centre of the contact. When the sphere is pressed against the flat, it deforms elastically and exerts a parabolic normal pressure distribution  $P$  (red parabola) on the liquid. In this state the contact resembles a parallel plate configuration and the confined liquid has roughly constant thickness throughout the contact. The hump is due to a reduction in film thickness, at the location of the pressure spike at the outlet of the contact (not shown) often associated with elastohydrodynamic lubrication. The molecular rotor ThT (spots in the figure) is added to the liquids Glycerol and IGEPAL. Its fluorescence intensity and lifetime increases with the viscosity of its surrounding as indicated by a halo (bright orange).  $a$  represents the radius of the contact and  $h$  is the film thickness separating the surfaces.

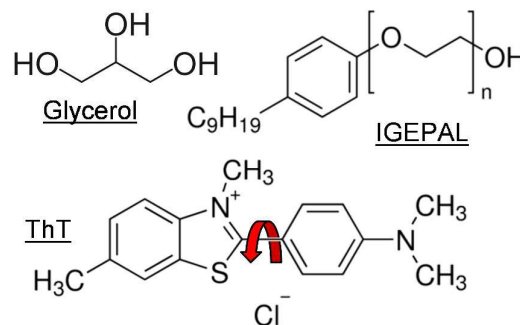


Fig. 2: Chemical structures of the liquids glycerol and IGEPAL as well as the dye ThT (red arrow indicates shared bond) used in this work

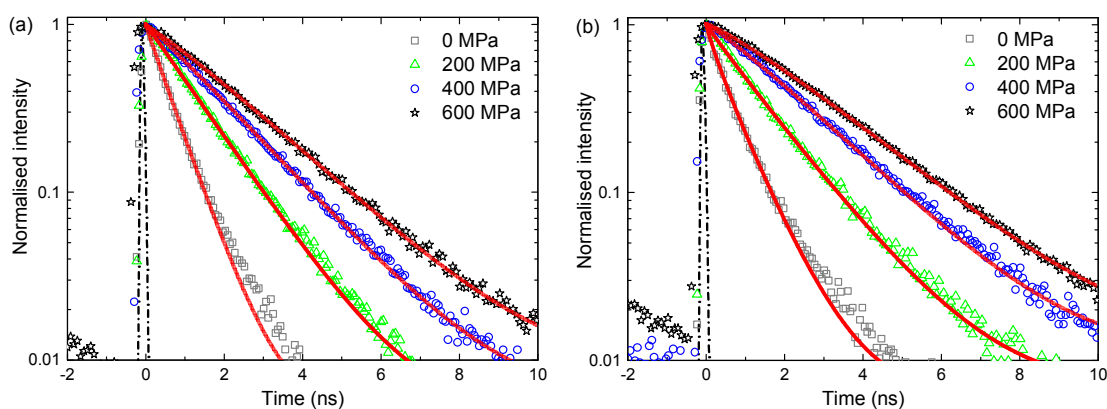
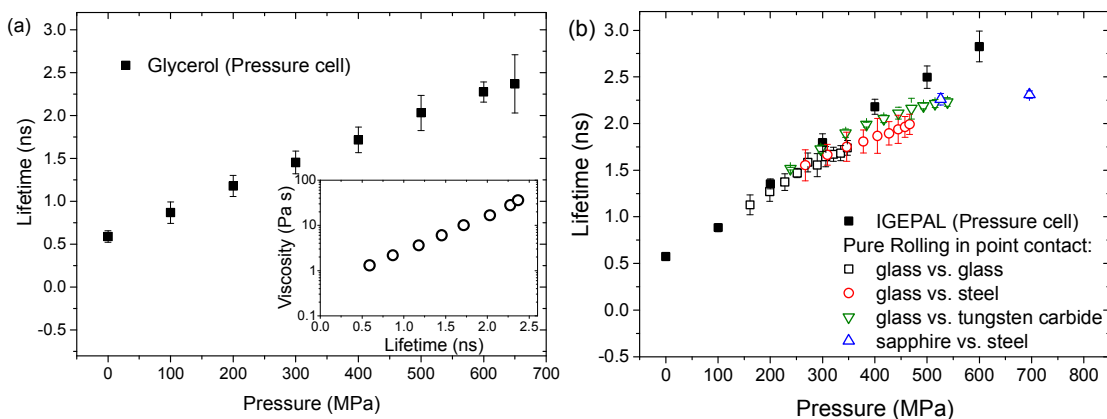


Fig. 3: Intensity response of ThT in glycerol (a) and IGEPAL (b) at various pressures measured using the pressure cell. The intensity was fitted to a stretched exponential (red lines) given by equation (3). The instrument response function (IRF) is shown as a dashed line. Stretched exponential fits to intensity decay are



shown as solid lines.

Fig. 4: (a) Calibration curve for glycerol showing the relationship between ThT lifetime and viscosity of glycerol. The insert shows how the lifetime of ThT changes with pressure obtained with the pressure cell. (b) The relationship between ThT lifetime in IGEPAL and applied pressure obtained with a pressure cell (filled squares) and at the centre of the contact under pure rolling conditions (thickness  $\approx$  140 nm) (unfilled symbols).

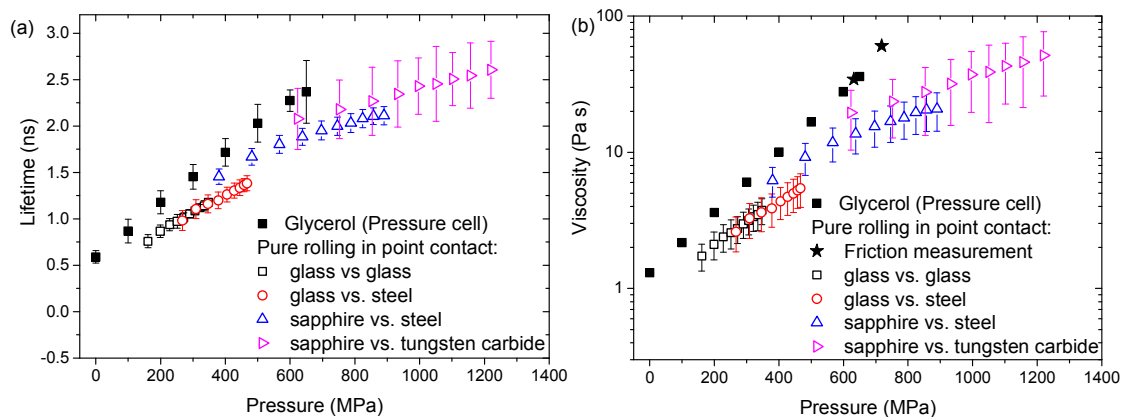


Fig. 5: (a) The ThT lifetime and (b) viscosity of confined glycerol at the centre of a point contact ( $u_e = u_b = u_d = 74 \text{ mm/s}$ ; shear rate = 0 and film thickness = 170 nm) obtained by ThT lifetime measurements (unfilled symbols) and of bulk glycerol in a pressure cell (filled squares).

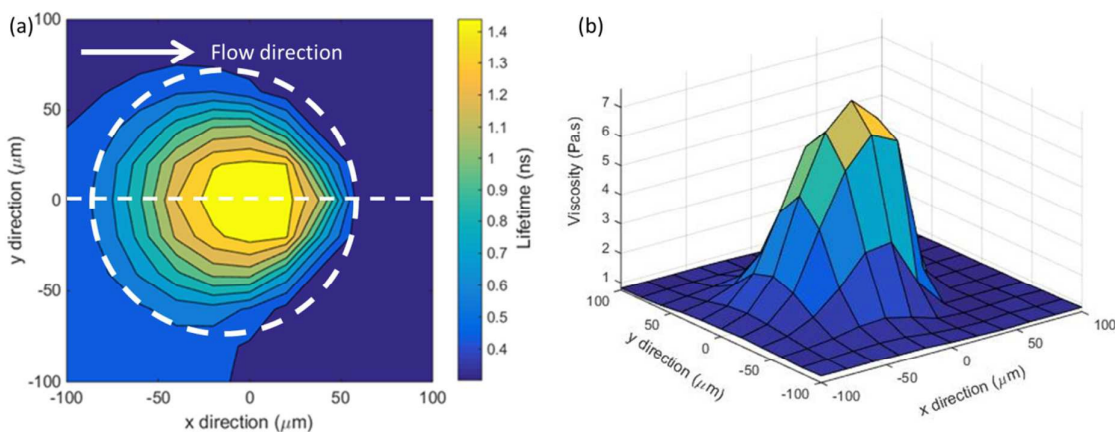


Fig. 6: (a) Variation of ThT lifetime in glycerol confined in a point contact. 121 data points in a grid of 11x11 was acquired and the data is plotted as a contour plot ( $P_{max} = 530 \text{ MPa}$ ,  $u_b = u_d = u_e = 74 \text{ mm/s}$ ,  $h = 170 \text{ nm}$ ). The white circle corresponds to the contact area ( $2a = 150 \mu\text{m}$ ). b) The corresponding viscosity map based on Fig. 6(a).



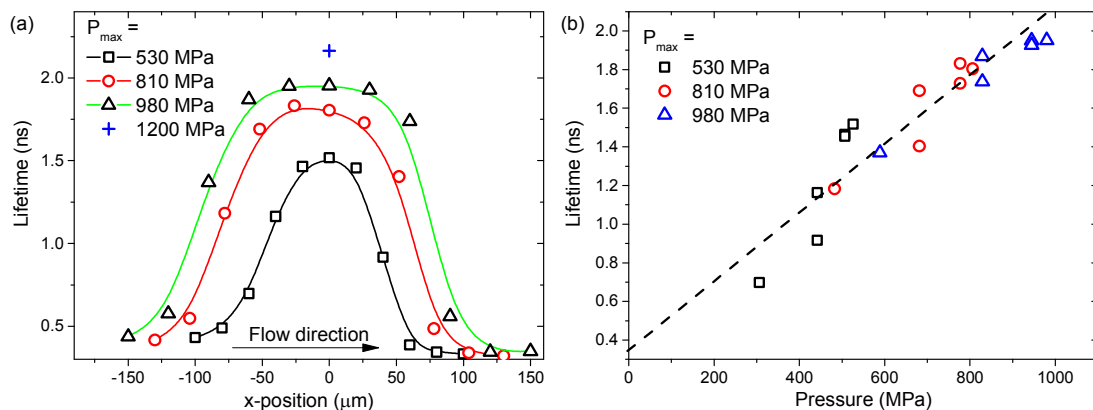


Fig. 7: (a) Variation of ThT lifetime in glycerol confined in a point contact at various loading conditions; (b) the effect of local pressure on ThT lifetime at various loading conditions. All lines are for guidance only

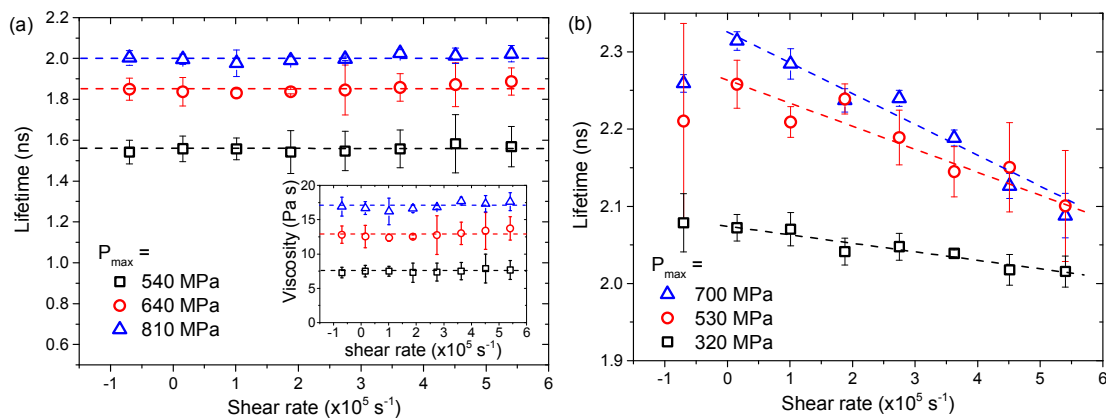


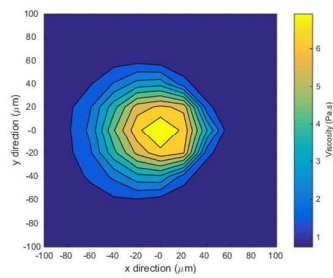
Fig. 8: (a) Variation of ThT lifetime in (a) glycerol and (b) IGEPAL; confined in a point contact at various shear rates. All lines are for guidance only.

**Journal Name**

ARTICLE

---

RSC Advances Accepted Manuscript



Viscosity heterogeneity in a thin glycerol film (170nm) at high pressure, high shear condition was observed with fluorescence lifetime measurement.